2025 IEEE Wireless Communications and Networking Conference (WCNC): 2025 IEEE Wireless Communications and Networking Conference (WCNC) Workshops

AFDM-based Integrated System for Underwater Detection and Communication Waveform Design

Qixiang Niu[a,b], Wentao Shi[a,c,*], David Ramírez[b,d], Lianyou Jing[c], and Qunfei Zhang[a]
[a] School of Marine Science and Technology, Northwestern Polytechnical University, Xi'an, 710072, China
[b] Department of Signal Theory and Communications, Universidad Carlos III de Madrid, Leganés, 28911, Spain
[c] Ocean Institute, Northwestern Polytechnical University, Taicang, 215400, China
[d] Instituto de Investigación Sanitaria Gregorio Marañón, Madrid, 28009, Spain
[*] Email: swt@nwpu.edu.cn

2025 IEEE Wireless Communications and Networking Conference (WCNC) | 979-8-3503-6836-9/25/$31.00 ©2025 IEEE | DOI: 10.1109/WCNC61545.2025.10978131

***Abstract*—Affine Frequency Division Multiplexing (AFDM) is an advanced communication waveform designed specifically for time-varying channels. This chirp-based multicarrier modulation technique is computationally efficient, which enables compact sonar implementations while achieving robust sensing performance through flexible parameter adjustments. Such characteristics make AFDM well-suited for Integrated Systems for Underwater Detection and Communication (ISUDC). In this paper, we explore an AFDM-based ISUDC system and propose a waveform model capable of transmitting multiple symbols to increase data capacity. We derive the Wideband Ambiguity Function (WAF) for this waveform and enhance it using complementary sequence coding, which reduces sensitivity to WAF variations and improves detection accuracy. Simulation results demonstrate that the proposed AFDM-based ISUDC waveform, featuring both multi-symbol support and complementary sequence coding, increases data capacity and improves communication bit error rate (BER) compared to traditional ISUDC waveforms. Additionally, the optimized WAF achieves enhanced detection performance, fulfilling critical ISUDC requirements.**

***Index Terms*—Affine frequency division multiplexing (AFDM), ambiguity function, complementary sequence code, integrated systems for underwater detection and communication (ISUDC), waveform design.**

I. Introduction

INTEGRATED Systems for Underwater Detection and Communication (ISUDC) have significant potential for applications such as smart ships, multi-base detection, among others. These systems have garnered considerable attention for their ability to combine detection and communication functionalities, which has ignited a lot of research in the coexistence, cooperation, and joint design of both functionalities. A central technology in ISUDC is the development of communication signal-centered waveforms that incorporate detection capabilities within the communication waveform itself, thereby enhancing detection performance to support reliable communication [1]. Achieving effective synergy between detection and communication functions first requires a thorough investigation of waveform detection performance and implementation of essential functionalities [2].

Affine Frequency Division Multiplexing (AFDM) has recently emerged as a multicarrier modulation technique based on chirp signals [3]. By extending modulation symbols across the entire time-frequency plane, AFDM achieves full diversity gain, making it particularly well-suited for communication in underwater, time-varying channel environments [4]. Traditional ISUDC waveforms, such as those based on Orthogonal Time-Frequency Space (OTFS) or Orthogonal Frequency Division Multiplexing (OFDM), have limitations, including suboptimal time-domain ambiguity functions and high computational complexity [5]. In contrast, AFDM's use of linear frequency modulation (LFM) signals, which are classic high-performance detection waveforms in radar and sonar applications [6], offers a natural integration of communication and detection functions. Given these characteristics, AFDM is highly capable of addressing the time-varying nature of underwater channels while effectively supporting ISUDC requirements [3].

However, while AFDM signals support both detection and communication functions, each pulse signal currently carries only one AFDM symbol, limiting the information-carrying rate within a fixed time period. Additionally, the Wideband Ambiguity Function (WAF) is a critical metric for assessing sonar detection performance, yet the presence of random communication data can affect the WAF, potentially degrading detection performance [7]. Therefore, there is a need to enhance both the information-carrying capacity of AFDM and its detection performance after modulation.

In this paper, we propose a scheme for modulating multiple AFDM symbols within a single transmit pulse to enhance the communication rate, resulting in a Multi-message Carrying AFDM (MCM-AFDM). We analyze the factors influencing the sensitivity of MCM-AFDM to communication information by deriving its WAF. To address this sensitivity, we introduce a complementary coding technique to encode communication data into complementary sequences. That is, we propose an improved MCM-AFDM waveform design algorithm incorporating complementary coding. In contrast, complementary coding MCM-AFDM (CCMCM-AFDM) employs complementary coding based on MCM-AFDM, leading to significant improvements in detection performance. The communication rate and bit error rate (BER) of the enhanced waveform are analyzed, and its underwater detection performance is demonstrated through WAF analysis.

979-8-3503-6836-9/25/$31.00 ©2025 IEEE

II. System Model

In this section, we focus on enhancing the communication capacity of a single AFDM pulse signal. We develop an AFDM-based waveform model, referred to as the Multi-message Carrying AFDM (MCM-AFDM) waveform, designed for use in ISUDC systems. Additionally, we study the underwater ambiguity function to assess the detection performance of the proposed system.

A. AFDM-based ISUDC Signal Waveforms

In the Discrete Affine Fourier Transform (DAFT) domain, let $\{a_n\}_{n=0}^{N-1}$ represent the communication data carried by each subcarrier, where N denotes the number of subcarriers. The AFDM transmitter generates the transmitted samples using an inverse DAFT (IDAFT) with parameters (c_1, c_2) [8], expressed as

$$s\left[k\right] = \frac{1}{\sqrt{N}} \sum_{n=0}^{N-1} a_n e^{j2\pi(c_2 n^2 + \frac{1}{N} nk + c_1 k^2)}, \tag{1}$$

where $k = 0, \ldots, N-1$. Similar to OFDM, AFDM adds a Chirp-Periodic Prefix (CPP) to the samples in (1) [3], which is given by $s[k] = s[N+k]e^{-j2\pi c_1(N^2+2Nk)}, k = -P, -P+1, \ldots, -1$, where P denotes the duration of the CPP. This duration must exceed the maximum delay of the communication channel and the maximum round-trip delay of the sonar target sampling. If $2c_1N$ is an integer and N is even, the CPP simplifies to a cyclic prefix (CP) [3].

Let $s(t)$ be the continuous-time counterpart of $s[k]$, which is given by

$$s(t) = \frac{1}{\sqrt{T}} \sum_{n=0}^{N-1} a_n e^{j2\pi(c_2 n^2 + \Phi_n(t))}, \tag{2}$$

where $T = N\Delta t$, Δt is the sampling period, and $2\pi\Phi_n(t)$ represents the instantaneous phase of the chirp, with $\Phi_n(t) = c_1' t^2 + \frac{n}{T} t$ and $c_1' = c_1/\Delta t^2$. The term $\Phi_n(t)$ can be divided into $C = 2c_1N$ windows within the time interval $[0, T)$, with separating times $\{t_{n,q}\}_{q=0,1,\ldots,C}$ given by $t_{n,0} = 0$ and $t_{n,q} = \frac{(N-n)}{2Nc_1}\Delta t + \frac{q-1}{2c_1}\Delta t$. This allows us to write [9]

$$\Phi_n(t) = c_1' t^2 + \frac{n}{T} t + \alpha_n(t), \quad t \in [t_{n,q}, t_{n,q+1}), \tag{3}$$

where $\alpha_n(t) = -\frac{q}{\Delta t} t$. Thus, (2) represents the waveform that carries a single message a_n per pulse, serving as the ISUDC signal for the duration of one pulse.

As demonstrated above, the AFDM signal transmits only a single AFDM symbol per pulse. Here, along the lines of previous works in OFDM/OTFS [10], we propose an enhanced AFDM-integrated signal that carries M communication symbols per pulse, denoted as the Multi-message Carrying AFDM (MCM-AFDM) signal, which can be expressed as

$$s(t) = \frac{1}{\sqrt{T}} \sum_{n=0}^{N-1} \sum_{m=0}^{M-1} a_{n,m} e^{j2\pi(c_2 n^2 + \Phi_n(t - m t_b))}, \tag{4}$$

where $a_{n,m}$ represents the communication data of the mth AFDM symbol modulated onto the nth subcarrier and t_b denotes the symbol duration. This signal waveform design increases the amount of communication data carried by the signal, thereby improving the communication efficiency of the ISUDC system.

B. Underwater wideband ambiguity function

The detection and estimation capabilities of a signal are typically assessed using its waveform ambiguity function. However, since hydroacoustic communication signals are often wideband, the design of ISUDC signal waveforms requires the wideband ambiguity function (WAF) [7], given by $\psi_{WAF}(\tau, \alpha) = |\chi(\tau, \alpha)|^2$, where $\chi(\tau, \alpha)$ is the two-dimensional autocorrelation function

$$\chi(\tau, \alpha) = \sqrt{\alpha} \int_{-\infty}^{\infty} s(t) s^*(\alpha(t - \tau)) dt, \tag{5}$$

and $\alpha = \frac{c - v_m}{c + v_m}$ is the Doppler factor, with c being the underwater speed of sound and v_m the radial velocity. Therefore, the analysis of the ambiguity function in the following sections will focus on $\chi(\tau, \alpha)$.

III. Complementary Coding Based on MCM-AFDM

A. Problem Formulation

This section obtains $\chi(\tau, \alpha)$ for the MCM-AFDM waveform in (4). Plugging (4) into (5) results in

$$\begin{aligned}\chi(\tau, \alpha) = &\\ &\frac{\sqrt{\alpha}}{T} \int_{-\infty}^{\infty} \sum_{n_1=0}^{N-1} \sum_{m_1=0}^{M-1} a_{n_1,m_1} e^{j2\pi(c_2 n_1^2 + \Phi_{n_1}(t - m_1 t_b))} \\ &\times \sum_{n_2=0}^{N-1} \sum_{m_2=0}^{M-1} a_{n_2,m_2}^* e^{-j2\pi(c_2 n_2^2 + \Phi_{n_2}(\alpha(t-\tau) - m_2 t_b))} dt,\end{aligned} \tag{6}$$

which can be divided into two components. The term corresponding to $n_1 = n_2$ is the self-ambiguity function $\chi_s(\tau, \alpha)$, which is the primary component of the ambiguity function. When $n_1 \neq n_2$, we get the cross-ambiguity function $\chi_c(\tau, \alpha)$, the secondary component that characterizes the neighborhood interference. Their expressions are, respectively,

$$\chi_s(\tau, \alpha) = \sum_{n=0}^{N-1} \sum_{m_1, m_2=0}^{M-1} a_{n,m_1} a_{n,m_2}^* \chi_{\Phi_n, \Phi_n}(\tau, \alpha, m_1, m_2), \tag{7}$$

and

$$\begin{aligned}\chi_c(\tau, \alpha) = &\sum_{\substack{n_1, n_2=0 \\ n_1 \neq n_2}}^{N-1} e^{j2\pi c_2(n_1^2 - n_2^2)} \\ &\times \sum_{m_1, m_2=0}^{M-1} a_{n_1,m_1} a_{n_2,m_2}^* \chi_{\Phi_{n_1}, \Phi_{n_2}}(\tau, \alpha, m_1, m_2),\end{aligned} \tag{8}$$

where

$$\chi_{\Phi_{n_1},\Phi_{n_2}}(\tau,\alpha,m_1,m_2) = \frac{\sqrt{\alpha}}{T}\int_{-\infty}^{\infty} e^{j2\pi[\Phi_{n_1}(t-m_1t_b)-\Phi_{n_2}(\alpha(t-\tau)-m_2t_b)]}dt. \quad (9)$$

It can be seen that the WAF of MCM-AFDM depends on the information data as shown in (7) and (8), which illustrate how $\chi_s(\tau,\alpha)$ and $\chi_c(\tau,\alpha)$ depend on the information symbols $a_{n,m}$. Additionally, they also determine the size of the peak when $\tau = 0$. That is, the information symbols determine the WAF in ISUDC. Ideally, the autocorrelation function of an information sequence should exhibit nonzero values only at its peaks, with all sidelobes reduced to zero [11]. This would achieve the optimal elimination of the sequence's impact on the WAF. Thus, the information sequence should fulfill

$$E\left[a_{n_1,m_1}a^*_{n_2,m_2}\right] = \begin{cases} 1, & n_1 = n_2, m_1 = m_2, \\ 0, & \text{otherwise.} \end{cases} \quad (10)$$

In practice, the transmitted data is determined by the source and often does not satisfy the condition in (10), resulting in a suboptimal autocorrelation function. For instance, consider the extreme case where identical symbols are transmitted, with each AFDM subcarrier carrying an all-ones sequence. This configuration leads to a poor correlation function, severely degrading the detection capabilities of the integrated system. Therefore, in MCM-AFDM modulation, the autocorrelation function of the message should be minimized to achieve a "pin-shaped" WAF. Using sequences with good correlation properties helps mitigate the impact of communication data on detection performance.

B. Complementary Sequence Coding

To obtain an information sequence with favorable correlation properties, thereby reducing the impact of MCM-AFDM communication data on detection performance and achieving a "pin-shaped" WAF, Golay sequences are typically considered. These sequences are encoded to generate codewords with a low peak-to-average ratio, suppressing signal peaks and minimizing the sensitivity of the message sequence on the WAF. Thus, we propose to encode communication messages as Golay complementary sequences [12].

Suppose $\mathbf{a} = (a_0, a_1, \ldots, a_{N-1})$ and $\mathbf{b} = (b_0, b_1, \ldots, b_{N-1})$ are binary sequences of length N, and define the acyclic autocorrelation function of the sequence $\mathbf{a}$ as

$$R_{\mathbf{a}}(k) = \sum_{l=0}^{N-k-1} a_l a_{l+k}, \quad (11)$$

with a similar definition of $R_{\mathbf{b}}(k)$. Then, sequences $\mathbf{a}$ and $\mathbf{b}$ are Golay complementary pairs (GCP) if

$$R_{\mathbf{a}}(k) + R_{\mathbf{b}}(k) = \begin{cases} 2N, & k = 0, \\ 0, & k \neq 0, \end{cases} \quad (12)$$

and either is called a Golay complementary sequence (GCS).

Linear packet codes (LPC) can be selected to generate GCSs, but it is desirable to select one with good error correction performance and that is easy to decode. In this paper, we shall use a Reed-Muller (RM) code as the error control code. Let $f(x_1, x_2, \ldots, x_d)$ represent a Boolean function corresponding to a binary code of length 2^d, with 2^d monomials matching the number of subcarriers in the MCM-AFDM signal, i.e., $N = 2^d$. The r-order binary RM code $\mathbf{R}(r,d)$ is constructed from the monomials of the Boolean function that are of at most rth order. Using this, the GCS can be derived from the RM codes [13], assuming that

$$f(x_1, x_2, \ldots, x_d) = 2^{h-1}\sum_{k=1}^{d-1} x_{\lambda(k)}x_{\lambda(k+1)} + \sum_{k=1}^{d} c_k x_k, \quad (13)$$

where λ represents an arbitrary permutation of the sequence $\{1, 2, \ldots, d\}$, with $\lambda(k)$ being the kth element of the sequence after permutation, x is the unit element of the generating matrix, h is the modulation depth, and c_k belongs to the set of integers of 2^h. Then, we can define

$$a(x_1, x_2, \ldots, x_d) = f(x_1, x_2, \ldots, x_d) + c, \quad (14)$$

$$b(x_1, x_2, \ldots, x_d) = f(x_1, x_2, \ldots, x_d) + 2^{h-1}x_{\lambda(1)} + c', \quad (15)$$

where c and c' belong to the set of integers 2^h, and the resulting sequences $\mathbf{a}$ and $\mathbf{b}$ are GCP of length 2^d.

Before proceeding, let us introduce the concepts of cosets and generating vectors in RM codes. A coset is defined as the set formed by the linear subspace of an RM code $\mathbf{R}(r,d)$ and its translations. In RM code decoding, coset partitioning is commonly used to identify the minimum Hamming distance, thereby facilitating the determination of the closest codeword. For an RM code $\mathbf{R}(r,d)$, its generating vectors are derived from all possible monomials of the d variables (up to degree r), which determine the structure and properties of the codewords.

Then, GCPs can be constructed from RM codes, with the first term being the coset generated by a first-order RM code of the form $2^{h-1}\sum_{k=1}^{d-1} x_{\lambda(k)}x_{\lambda(k+1)}$ of the head of the coset, and the second and third terms consisting of linear combinations of the generating vectors of the first-order RM code. There are a total of $\frac{d!}{2}$ heads, and a total of 2^{d+1} linear combinations of $\mathbf{R}(1,d)$. Consequently, the $\frac{d!}{2}2^{d+1}$ GCS can be constructed from the $\mathbf{R}(2,d)$ vector matrix.

In complementary sequence coding, the first element of the accompanying set is determined based on the number of subcarriers

$$\omega = \left\lfloor \log_2\left(\frac{d!}{2}\right)\right\rfloor, \quad (16)$$

where $\lfloor\cdot\rfloor$ denotes the floor operator and M becomes

$$M = \omega + h(d+1). \quad (17)$$

The corresponding head of the coset is obtained using the first information bit and the matrix formed by it is called the

head of the coset matrix $\mathbf{H}$. Hence, the head of the coset vector can be expressed as

$$\mathbf{g} = \mathbf{H}\left(L+1,:\right), \tag{18}$$

where L is the integer obtained by transforming the vector of information bits $\mathbf{x} = (x(1), x(2), \ldots, x(\omega))$ to a decimal number of the set 2^h. The next step is to convert $h(d+1)$ bits into $d+1$ symbols in base 2^h, and then linearly combine them with the generation vector to obtain the vector $\mathbf{q}$. Adding these two components $\mathbf{q}$ and $\mathbf{g}$ results in the CCMCM-AFDM subcarrier data encoded with the Golay sequence, as detailed in steps five and six of Alg. 1. The complete CCMCM-AFDM technique is summarized in Alg. 1 .

Algorithm 1 CCMCM-AFDM Waveform Algorithm

Input: N, d, T, t_b, h, $\mathbf{x}$, $\mathbf{H}$, $R_{2^h}(1,d)$ generating matrix $\mathbf{R}$
Output: $s(t)$

1: Compute M using (17), ω using (16), h, and d;
2: Compute L from $\mathbf{x} = (x(1), x(2), \ldots, x(\omega))$;
3: Compute $\mathbf{H}$ and head vector $\mathbf{g}$ using (17);
4: **for** $i = 0, \ldots, d$ **do**
5: Information bits $x(\omega{+}1{+}ih), x(\omega{+}2{+}ih), \ldots, x(\omega{+}(1+i)h)$ are converted to the integer form of the sequence c_{i+1};
6: Compute the composition of linear combinations of the generating vectors, $\mathbf{q} = \mathbf{q} + c_{i+1}\mathbf{R}(i+1,:)$;
7: **end for**
8: Compute the complementary coding $\mathbf{e} = (2^{h-1}\mathbf{g} + \mathbf{q})$;
9: Compute the CCMCM-AFDM waveform $s(t)$ using (4), N, M, $\mathbf{e}$, T, and t_b, where the elements in $\mathbf{e}$ are the symbols $a_{n,m}$.

IV. Numerical Results

The system simulation parameters in this section are: carrier frequency $f_c = 20$ GHz, subcarrier spacing $\Delta f = 156.25$ kHz, the number of CCMCM-AFDM subcarriers $N = 64$, and the number of AFDM symbols are $M = 64$, so that the system has a bandwidth of $N\Delta f = 10$ MHz and a pulse width $T = 1/\Delta f = 6.4$ μs, and $t_b = 0.1$ μs. AFDM is an ideal waveform for ISUDC when $c_2 = 0$ [3], which is the value adopted in this paper . The underwater acoustic velocity $c = 1500$ m/s, and the radial velocity v_m varies from -10 m/s to 10 m/s. In the following experiments, four sets of information sequences were modulated using two different methods to verify the improvement in WAF obtained from the complementary sequence coding. Two of the information sources were specially designed sequences, while the other two were randomly generated sequences. These are depicted in Fig. 1.

In the first experiment, Fig. 2 presents the ambiguity function plots, time-delay variations, and radial velocity trends for the CCMCM-AFDM and MCM-AFDM signals for Sequence 3. Both signals carry the same information; however, the latter lacks complementary sequence coding. As the figure shows, the WAF of the MCM-AFDM signal displays a triangular envelope, particularly evident in the zero-delay plot. In this case, the small difference between the main spike and the sidelobes complicates accurate target identification, as high sidelobe peaks obscure detection. Conversely, the WAF of the CCMCM-AFDM signal exhibits a "pin-like" shape, decaying rapidly in all directions. This structure enables high resolution in both radial velocity and time delay. Notably, the spike-to-sidelobe difference in the zero radial velocity map is approximately 40 dBs, offering significantly improved distance resolution compared to MCM-AFDM. Furthermore, the zero time-delay map closely resembles that of the linear FM signal, with complementary sequence coding enhancing detection performance in both cases.

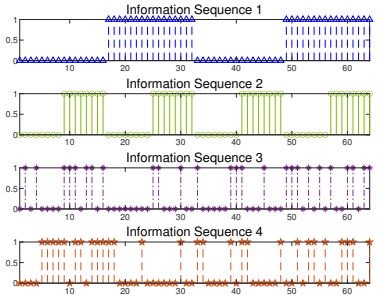

Fig. 1. Four generated information sequences

Figures 3 through 6 illustrate the WAFs of MCM-AFDM and CCMCM-AFDM signals for the four different information sequences of Fig. 1. Specifically, Fig. 3 shows the delay slice of the WAF for the MCM-AFDM waveform at $\alpha = 0$, while Fig. 4 presents the Doppler slice at $\tau = 0$. As observed, the ambiguity functions of Sequence 1 and Sequence 2 lack prominent main peaks and exhibit relatively uniform peak heights. This uniformity makes it difficult to distinguish the target among multiple peaks during detection. In contrast, Figs. 5 and 6 depict the WAFs of CCMCM-AFDM signals after applying complementary sequence coding, shown at both zero Doppler and zero delay. For all sequences, these WAFs exhibit a distinctive "pin-like" shape, characterized by a sharp main peak and rapid decay in all directions. This structure ensures high resolution in both radial velocity and time delay, significantly outperforming the original MCM-AFDM modulation waveform.

The results confirm that the ambiguity function of the original MCM-AFDM waveform is highly sensitive to the information it carries, particularly in extreme cases such as Sequences 1 and 2, where continuous blocks of zeros or ones are present. This sensitivity compromises detection performance. In contrast, as illustrated in Figs. 5 and 6, the application of complementary sequence coding significantly enhances robustness. Even under the challenging conditions posed by Sequences 1 and 2, the resulting ambiguity functions maintain high resolution in both time delay and Doppler.

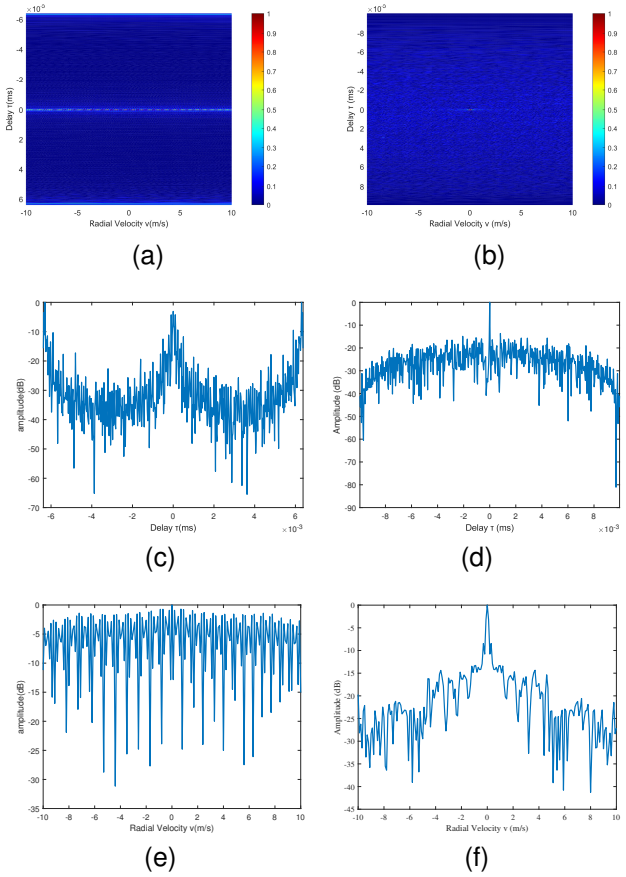

Fig. 2. (a)(c)(e) are WAF plots, zero radial velocity plots, and zero delay plots for MCM-AFDM; (b)(d)(f) are WAF plots, zero radial velocity plots, and zero delay plots for CCMCM-AFDM

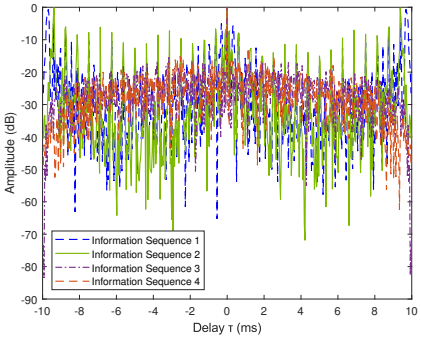

Fig. 3. The zero radial velocity plot of the WAF for MCM-AFDM.

These findings demonstrate that complementary sequence coding effectively accommodates various source sequences while ensuring reliable and consistent detection performance.

The coding rate is also an important factor in evaluating the communication performance of the ISUDC waveform, as it measures the efficiency of transmitting useful information. The coding rate is defined as the ratio of the number of information bits to the number of coded bits. It is influenced by the coding length d and the baseband modulation depth h,

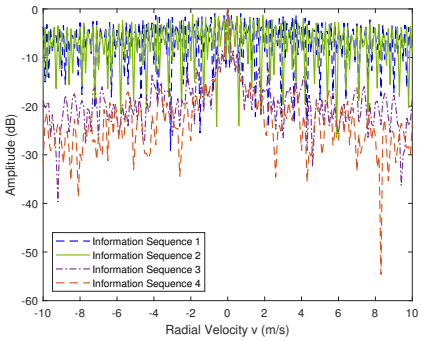

Fig. 4. The zero time delay plot of the WAF for MCM-AFDM

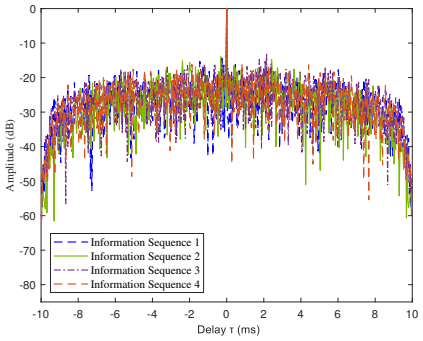

Fig. 5. The zero radial velocity plot of the WAF for CCMCM-AFDM.

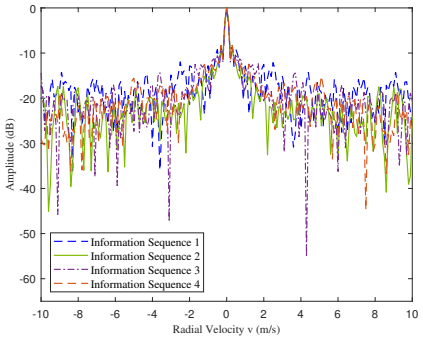

Fig. 6. The zero time delay plot of the WAF for CCMCM-AFDM.

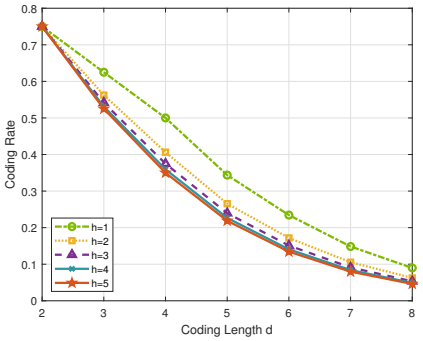

Fig. 7. CCMCM-AFDM coding rate with modulation depth and coding length

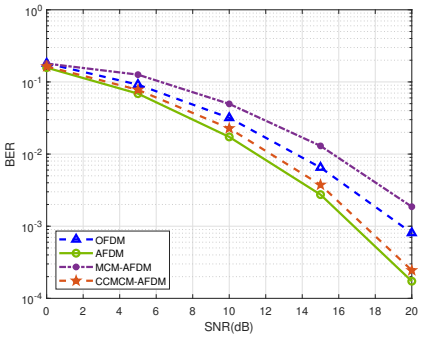

Fig. 8. BER Performance Comparison of AFDM, MCM-AFDM and CCMCM-AFDM

and the relationship can be expressed as

$$R_D = \frac{\omega + h(d+1)}{2^d \cdot h}. \tag{19}$$

The relationship between the coding rate of CCMCM-AFDM, coding length, and baseband modulation depth is illustrated in Figure 7. It is evident that the coding length significantly influences the coding rate, while the impact of modulation depth is relatively minor. For instance, when $h = 3$ and $d = 4$, the number of CCMCM-AFDM subcarriers is 16, yielding a coding rate of 0.375. Selecting $d = 5$ reduces the coding rate to 0.239. This indicates that the algorithm is more suitable for scenarios with a smaller number of subcarriers.

Finally, we assess the impact of the proposed technique on communication performance. Figure 8 presents the bit error rate (BER) of MCM-AFDM and CCMCM-AFDM modulated waveforms under identical data loads and system parameters. The results are compared to those of the original AFDM signal and the commonly used ISUDC waveform based on OFDM [10]. The BER of the CCMCM-AFDM waveform closely matches that of the original AFDM signal and outperforms the OFDM waveform. In contrast, the MCM-AFDM signal exhibits inferior communication performance compared to both OFDM and CCMCM-AFDM signals. These findings demonstrate that the improved CCMCM-AFDM with complementary sequence coding not only enhances detection performance but also maintains BER levels comparable to AFDM, achieving a favorable balance between detection and communication performance.

V. Conclusion

This paper proposes a novel waveform design algorithm for ISUDC systems based on AFDM, introducing the MCM-AFDM waveform, which incorporates multiple AFDM symbols within each pulse to enhance communication capacity. To address detection degradation caused by unoptimized coding, complementary sequence coding is applied, improving detection performance by optimizing the waveform ambiguity function. The resulting CCMCM-AFDM waveform ensures robust range and time-delay resolution under extreme conditions while maintaining reliable communication performance. Simulations show that the proposed waveform achieves a bit error rate comparable to traditional AFDM, outperforming OFDM and MCM-AFDM, and effectively balances detection and communication, making it ideal for integrated underwater sensing and communication systems.

Acknowledgment

This study was supported by the National Natural Science Foundation of China (NSFC) under Grant No. 62371393. The work of D. Ramírez was partially supported by MICIU/AEI/10.13039/501100011033/FEDER, UE, under grant PID2021-123182OB-I00 (EPiCENTER), by the Office of Naval Research (ONR) Global under contract N62909-23-1-2002, and by the Spanish Ministry of Economic Affairs and Digital Transformation and the European Union-NextGenerationEU through the UNICO 5G I+D SORUS project.

References

[1] M. F. Ali, D. N. K. Jayakody, Y. A. Chursin, S. Affes, and S. Dmitry, "Recent advances and future directions on underwater wireless communications," *Archives of Computational Methods in Engineering*, vol. 27, pp. 1379–1412, 2020.

[2] S. F. Mason, C. R. Berger, S. Zhou, and P. Willett, "Detection, synchronization, and Doppler scale estimation with multicarrier waveforms in underwater acoustic communication," *IEEE Journal on Selected Areas in Communications*, vol. 26, no. 9, pp. 1638–1649, 2008.

[3] A. Bemani, N. Ksairi, and M. Kountouris, "Affine frequency division multiplexing for next generation wireless communications," *IEEE Transactions on Wireless Communications*, vol. 22, no. 11, pp. 8214–8229, 2023.

[4] J. Zhu, Q. Luo, G. Chen, P. Xiao, and L. Xiao, "Design and performance analysis of index modulation empowered AFDM system," *IEEE Wireless Communications Letters*, 2023.

[5] Y. Han, L. Wang, L. Xu, W. Zhu, Y. Zhang, and A. Fei, "Pilot optimization for OFDM-based ISAC signal in emergency IoT networks," *IEEE Internet of Things Journal*, 2023.

[6] N. Zhong, P. Li, W. Bai, W. Pan, L. Yan, and X. Zou, "Spectral-efficient frequency-division photonic millimeter-wave integrated sensing and communication system using improved sparse LFM sub-bands fusion," *Journal of Lightwave Technology*, 2023.

[7] C. Liu, Y. V. Zakharov, and T. Chen, "Broadband underwater localization of multiple sources using basis pursuit de-noising," *IEEE Transactions on Signal Processing*, vol. 60, no. 4, pp. 1708–1717, 2011.

[8] S.-C. Pei and J.-J. Ding, "Closed-form discrete fractional and affine Fourier transforms," *IEEE Transactions on Signal Processing*, vol. 48, no. 5, pp. 1338–1353, 2000.

[9] A. Bemani, N. Ksairi, and M. Kountouris, "Integrated sensing and communications with affine frequency division multiplexing," *IEEE Wireless Communications Letters*, vol. 13, no. 5, pp. 1255–1259, 2024.

[10] Q. Wang and P. Fan, "A multi-symbol compressive sensing model for OTFS based ISAC system," in *2023 IEEE Global Communications Conference (GLOBECOM)*, 2023, pp. 2487–2492.

[11] W. Wei and Y. Wei, "Unimodular sequence set design for mimo radar ambiguity function shaping," in *2023 IEEE Radar Conference (RadarConf23)*, 2023.

[12] M. Waegell and P. K. Aravind, "Golay codes and quantum contextuality," *Physical Review A*, vol. 106, no. 6, p. 062421, 2022.

[13] E. Abbe, O. Sberlo, A. Shpilka, and M. Ye, "Reed-Muller codes," *Foundations and Trends® in Communications and Information Theory*, vol. 20, no. 1–2, 2023.